ON THE FRICTIONAL RESISTANCE OF ENCLOSED ROTATING DISC OF VARIOUS SURFACES

KŌMEI WATABE

Department of Mechanical Engineering

(Received May 31, 1962)

1. Introduction

Although numerous studies of disc friction have been already carried out by Kármán[1], Schultz-Grunow[2], Pantell[3], Fujimoto and Iwagaki[4], J. W. Daily and R. E. Nece[5] and others, detailed experiments on discs or vessels which have sand-grains or protuberances on their surfaces have not yet been performed.

The author carried out a series of experiments on the frictional resistance of enclosed rotating discs. Many combinations of rotating discs and vessels with various surface conditions are taken: smooth or rough grained or bladed surface. The "bladed" surface consists in the arrangement of protuberances. He also discussed the influences of height, size of the rough grains and the blades, and of axial clearances on the fluid friction.

2. Experimental equipment and procedure

Fig. 1 is a sketch of the experimental equipment. Resisting moment of the disc is found by measuring the torsional deflection in a helical spring. The resisting moment induced by the bearing, air friction is measured by rotating the shaft without disc. Then the net resistance of the disc by fluid friction is the difference between the resisting moment obtained directly by experiments and the resisting moment by bearings etc.

In order to guard against an overflowing of the liquid from the vessel, a rubber packing must be inserted in the center of the upper plate of the vessel. The resistance between the packing and the shaft of disc is little.

In our experiment, the axial clearance is about 0.75~17.50 mm and can be changed by using different lengths of cylinder. Since the disc should be located in the middle of vessel, whenever we exchange cylinder, we must move the vessel up or down by adjusting the screws supporting the vessel, and we check the magnitude of axial clearances by reading the indications of three gauges which are installed in small holes in the upper plate, respectively.

Radial clearance t is 1.0~55.0 mm, and can be changed by using discs of different diameters.

For smooth surface experiment, the disc surface, upper and lower plates, and the inner surface of cylinder are made of polished nickel, and for rongh surface experiments, all surfaces are covered with grains of sand. Coarse sand grains are obtained by sifting river sand through "standard mesh" and fine sand grains are obtained by the precipitation method of Stokes. Before starting the experiment, we check the grain size by microscope. Magnitudes of grains are shown

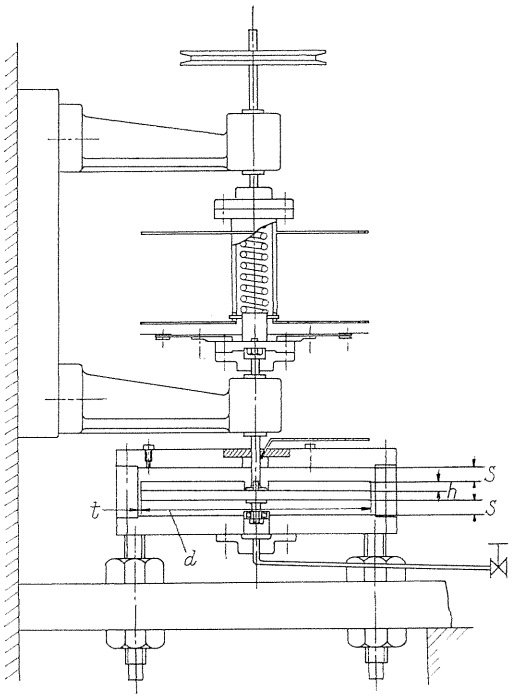

FIG. 1. Experimental apparatus.

TABLE 1. Classification of Grains

Note	Way of selection	Grain materials	Mean dia. of grain in mm
I	Sifting method (42~ 45 mesh)	River-sand	0.34
II	〃 (80~100 mesh)	〃	0.16
III	〃 (150~170 mesh)	〃	0.10
IV	Precipitating method	〃	0.04
IV_f	〃	Fly-ash	0.04
V_f	〃	〃	0.02
VI	〃	River-sand	0.01

in Table 1, where IV_f and V_f represent grains of fly-ash, spherical in shape and entirely different from the shape of river sands. The mode of finishing rough surface is quite important as the size and shape of the grain itself. Hence we must always be careful to attach the sand under the same condition, and we used "Melamin" of suitable viscosity as an adhesive of liquid.

In addition, we experiment with the bladed surfaces. The blades are arranged concentrically or radially on the surface of discs. The radial blades has width $a=5.0$ mm and height $h=3.0$, 6.0, 12.0 mm and length $l=115.0$, 103.0, 78.0 mm. They are fixed on one side of disc surfaces and have rectangular sections. As the number of blades Z increases ($Z\geqq 16$), the circular interval of blades becomes zero in the center of disc. Then, in the case of Z greater than 16, the shorter blades are fixed in each space of blades previously fixed, and the space of disc center between these blades is filled with solder, consequently a smooth surface

of dia. 102.0 mm (for $Z=64$). Furthermore, several blades were fixed on the surface of the vessel, concentrically and radially, as in the following section. The several blades used here are classified in Table 2. Experiments are carried out in combination of the bladed disc and the smooth vessel, the smooth disc and the bladed vessel and moreover both the bladed disc and the vessel. In each combination experiments are carried out for various axial clearances s.

TABLE 2. Classification of Blades

Disc or vessel→	Disc (dia.: 258.0 mm)					Vessel (ins. dia.: 261.0 mm)				
Dimensions of blades ↓	Radial blades			Concentrical blades		Radial blades		Concentrical blades		
Height h mm	3.0	6.0	12.0	3.0	3.0	3.0	6.0	3.0	3.0	3.0
Width a mm	5.0	5.0	5.0	5.0	90.0	5.0	5.0	65.0	2.5 22.5	2.5
Number Z	2, 4, 8, 12, 16, 32, 64	2, 4, 8, 16, 32, 64		1, 2	1	4, 8	2, 4, 8	1	2	1, 2
Length l mm	115.0 (103.0, 78.0)			—		115.0		—		

3. Experimental results and considerations

The resisting moment of a rotating disc is generally given by the following expression,

$$M=C_f \cdot \rho \cdot \omega^2 \cdot r^5 \tag{1}$$

where M: resisting moment, ρ: density of fluid, ω: angular velocity of disc, r: disc radius, C_f: coefficient of frictional resistance.

We can express C_f as a function of R_e, s/d, t/d, i/d, Z, h, etc., where R_e: Reynolds number ($=\omega r^2/\nu$), ν: kinematic viscosity, s: axial clearance, t: radial clearance, i: diameter of grain, d: diameter of disc, Z: number of blades, h: height of blades.

In our numerous experiments, we were able to find the relation between C_f and R_e by using parameter s/d, where t/d and i/d are kept constant, and also the relation between C_f and i/d by using R_e as a parameter where s/d and t/d are constant. In our experiments using water and glycerine, the region of R_e is within $10^5 \sim 10^7$.

3.1. Experiments of smooth disc in smooth vessel

Firstly, we give results of the experiments on smooth surfaces of both disc and vessel ($i=0$) in order to compare experimental results of rough and smooth surfaces. When the radial clearance ratio t/d is held constant and axial clearance ratio s/d is varied, experimental results are as given in Fig. 2. When s/d is constant and t/d is changed, results are as in Fig. 3. In all the diagrams in the present paper, the line A expresses the relation between C_f and R_e for turbulent flow, and the line B represents that for laminar flow, and the relation of the lines

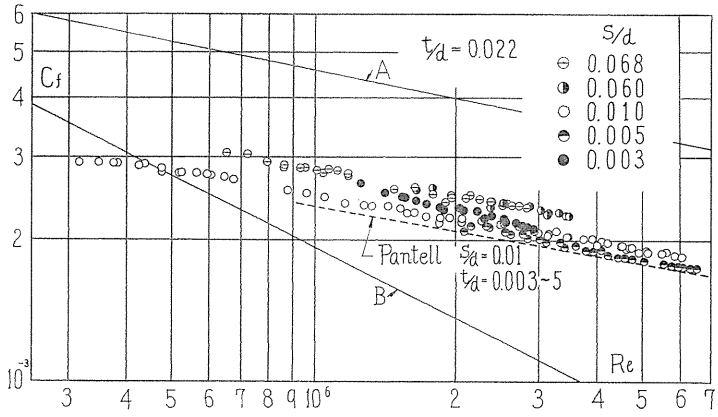

FIG. 2. Influence of s/d on smooth disc in smooth vessel.

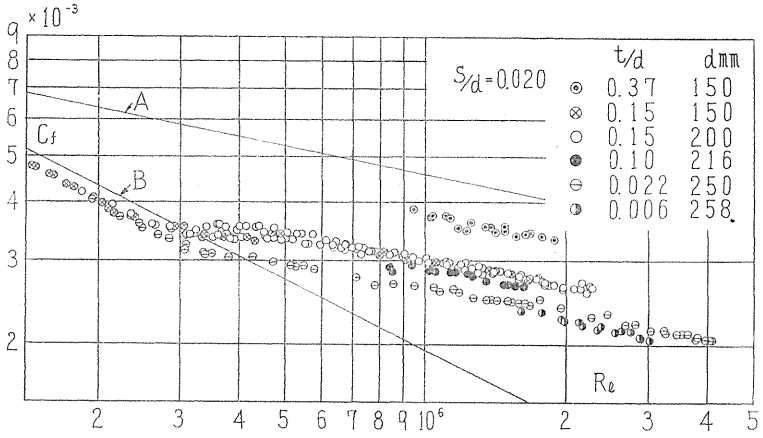

FIG. 3. Influence of t/d on smooth disc in smooth vessel.

A and B are obtained by Kármán's theoretical calculation. Equations of the lines A and B are given by $C_f = 0.0728\ R_e^{-1/5}$ and $C_f = 1.935\ R_e^{-1/2}$, respectively. In the region of laminar flow, lines indicating the relation between C_f and R_e obtained by experiments are in parallel with the line B, and we see that no influence of axial and radial clearances t and s appears. In the region of turbulent flow beyond $R_e = 6 \times 10^5$, lines are almost in parallel with the line A, and the values of C_f increase with magnitudes of s and t, with one exception, that for a special value of clearance $s/d = 0.003$.

In Figs. 4 (a) and (b), the curves $C_f - s/d$ and $C_f - t/d$ with parameter R_e are shown. Observing Fig. 4 (a), we can see that there is a special value of clearance just mentioned. In Fig. 4 (a), values, C_f become large with axial clearances and approach asymptotically to a certain value which is particular to the value of s. In Fig. 4 (b), however, the relation between C_f and R_e can be represented by straight lines. From Fig. 4 (a), we can find that the resistance coefficient C_f

takes a minimum value for a certain value of clearance $s/d=0.005$, and increases steeply when the clearance becomes smaller than this special value.

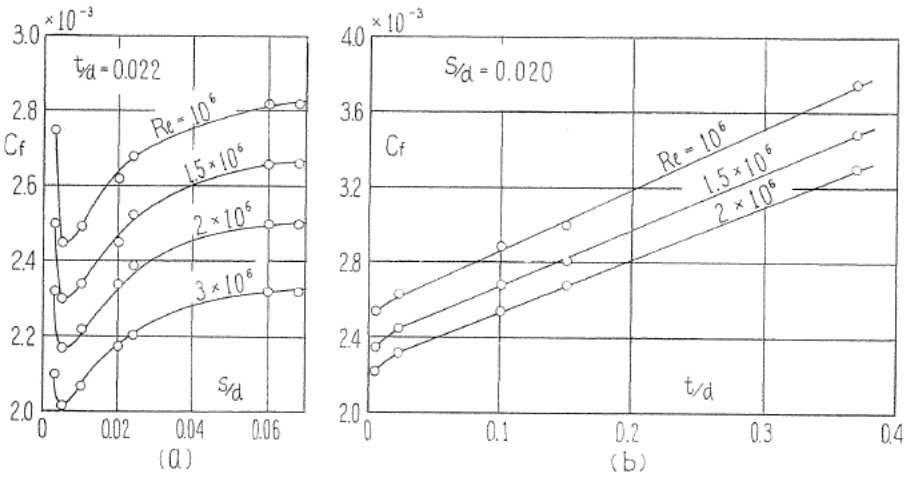

FIG. 4. Curves C_f-s/d, C_f-t/d.

In Fig. 2, the broken line curve is that given by Pantell's empirical formula

$$K_s = 0.9\frac{1}{(s/d)^2(R)^{1,2}} + \frac{0.51+s/d}{(3.0+s/d)\cdot 5\cdot (R)^{0,182}}$$

$$K_s = \frac{5}{2\pi}C_f, \quad R = \frac{30}{\pi}R_e \tag{2}$$

which almost coincides with our experimental results. Since, in Fig. 3, experimental results for $d=150$ mm coincide with those for $d=200$ mm, we can conclude that resistance coefficient C_f can be represented by only Reynolds number R_e, provided that geometrical similarity is held.

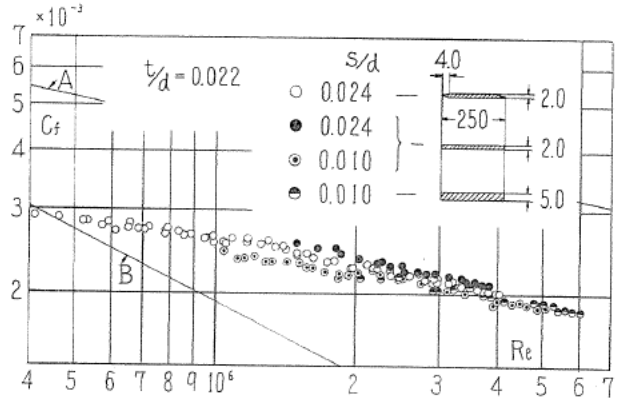

FIG. 5. Influence of cylindrical surface of disc.

In order to examine the influence of cylindrical surface of discs we carried out experiments as shown in Fig. 5. The value of C_f, when the disc has a sharp edge, is smaller than that when the disc has a cylindrical surface. Furthermore, the magnitude of area of the cylindrical surface of the disc has no influence on the value of C_f. The facts just mentioned above may be the result of a secondary flow in vessel induced by the rotating disc.

3.2. Effects of rough grains

3.2.1. Experiments of smooth disc in rough vessel

The experimental results when the disc has smooth surfacs and the vessel has rough surface are given in Fig. 6. The resistance coefficiennt C_f shown in Fig. 6 is obviously larger than that of smooth surface. In laminar flow region, curves C_f-R_e are in parallel with the line B for all rough surfaces, as experimental results shown in Fig. 6. In the turbulent flow region, they also tend to be parallel with the line A. In Fig. 6, C_f has large value with increasing roughness i/d. Transitional region between laminar and turbulent flows is more expansive than when the vessel surface is smooth.

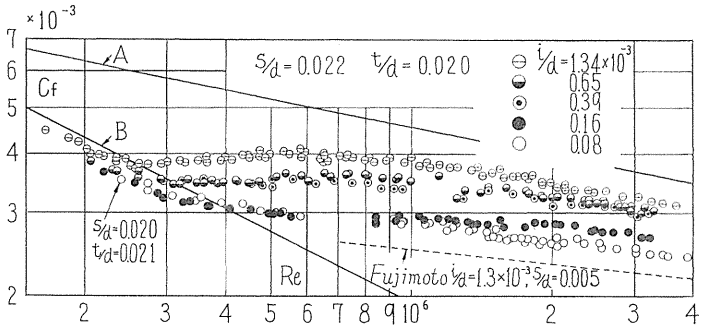

FIG. 6. Results for smooth disc in rough vessel.

The broken line indicated in Fig. 6 represents the values of C_f obtained theoretically by Fujimoto and Iwagaki's formula

$$C_f=0.00791\{R_e\cdot(s/r)^2\cdot r/i\}^{-0.1091} \tag{3}$$

which is given for the case of smooth disc and rough vessel and vise versa, when axial clearance is very small. The value C_f given by (3) is considerably smaller than that obtained from our experiment.

3.2.2. Experiments of rough disc in smooth vessel

The resistance coefficient C_f is larger than that when the disc is smooth and the vessel is rough, as shown in Fig. 7. The value of R_e at which the transition region between laminar and turbulent flow begins to appear, become smaller with the increase of roughness. The curve indicated by the symbol ① in Fig. 7 represents the result caused by an unskilled way in which sand-grains were attached. Obviously the value given by this curve is smaller than that furnished

by well fixed grains of the same size, indicated by the symbol ⊖ in Fig. 7. Additionally, we find no influence of the shape of sand-grains on C_f by either river-sand or fly-ash, because these two different kinds of sand-grains give the same value of C_f, as shown in Fig. 7.

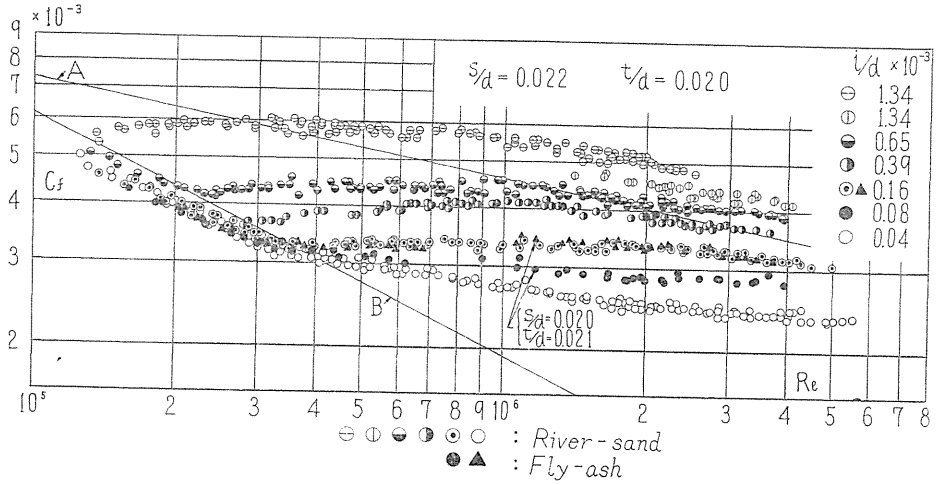

FIG. 7. Results for rough disc in smooth vessel.

3.2.3. Experiments of rough disc in rough vessel

Result from the experiments with discs of several different roughness in rough vessel of grain V_f (diameter i=0.02 mm) are given in Fig. 8. In the neighborhood of $R_e=2\sim3\times10^5$, C_f is independent of R_e and tends to a certain value as R_e increases. For comparison, in Fig. 8 the results of experiments in smooth vessels as shown in Fig. 7 are reproduced in broken lines ①, ②, ... Accordingly, the influence of vessel of roughness V_f does not appear untill R_e reaches about 4×10^5.

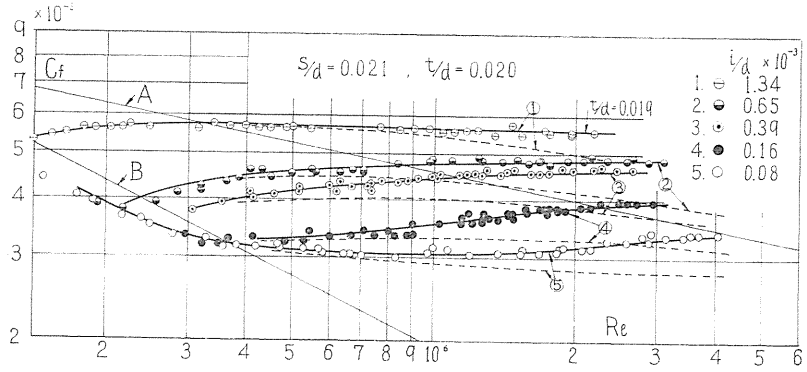

FIG. 8. Results for rough disc in rough vessel. (1)

Furthermore, experimental results given by suitably arranged discs and vessels of different roughness are shown in Fig. 9. We use, as an example, a notation [II-II] where in this bracket the former numeral represents roughness of disc and the latter roughness of vessel (see Table 1). Note that 0 means smooth surface. Symbols [I-IV] and [II-II] have resistance coefficients of nealy the same values under the same conditions of s/d and t/d; hence they are equivalent roughness in the sense of hydraulics.

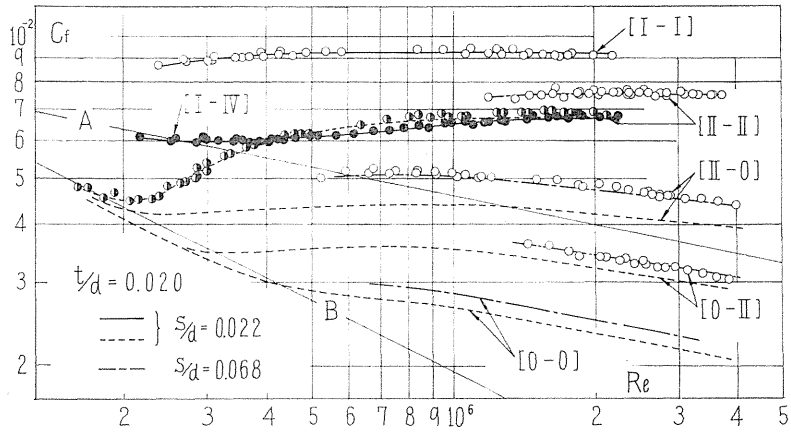

FIG. 9. Results for rough disc in rough vessel. (2)

The difference between broken lines ($s/d=0.022$) and chain lines ($s/d=0.068$) for the case of [II-II] is equal to that of [II-0]; for the case of [0-II] is equal to that of [0-0], and the difference of [II-II] and [II-0] is nearly twice that of [0-II] and [0-0]. From this fact, we may see, on one hand, that the degree of influence of clearance is only slightly affected by the degree of rouhness of vessel, and we see that it depends on roughness of disc, on the other. In the above results, the relationship between C_f and i/d are given by the following expression

$$C_f=0.126\ (i/d)^{2/5} \tag{4}$$

for small axial clearance ($s/d=0.022$).

3.3. Effects of concentrical blades

Blades are fixed concentrically on the inside of the vessel or only in the upper side of discs, the sections of which are as shown in the right corners of Fig. 10, Fig. 11, respectively. Heights of the blades are all $h=3.0$ mm. Axial clearance s is taken as the distance between the upper (or lower) edge of blades and the smooth surface of disc (or vessel).

Fig. 10 shows the experimental results of smooth disc in bladed vessel for $s/d=0.018$ and $s/d=0.004$. I, VI are the results of smooth disc in smooth vessel. Results II~V lies between I and VI, when $R_e>10^6$, and almost in parallel with the line A (see section 3.1.). On the whole, no obvious difference is seen in them in the author's experimental region, but the line V shows approximately

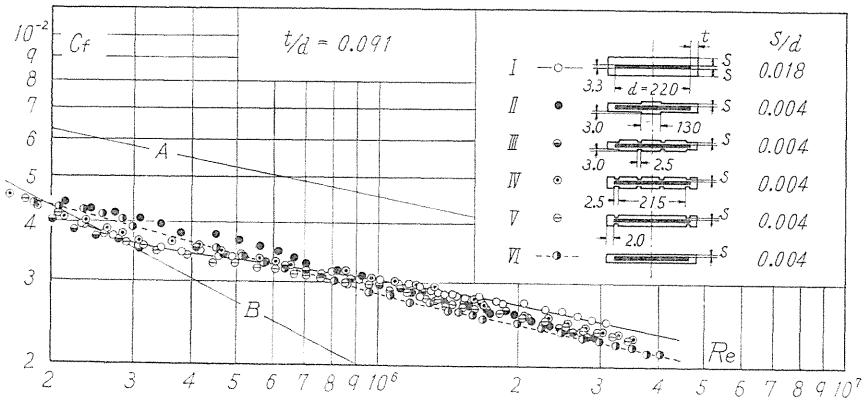

FIG. 10. Results for smooth disc in concentrically bladed vessel.

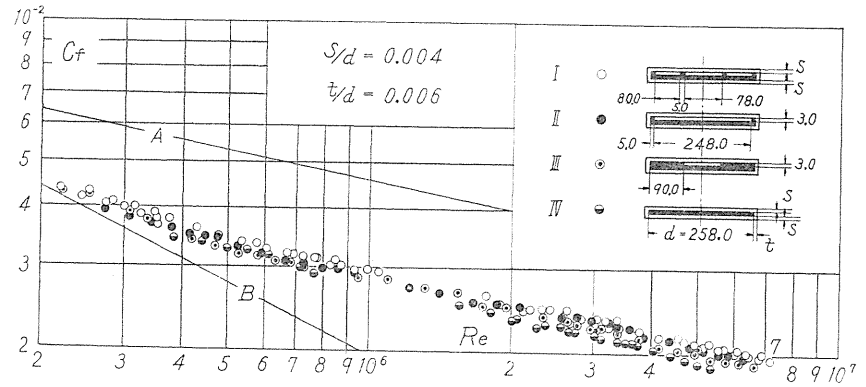

FIG. 11 (a). Results for concentrically bladed disc in smooth vessel (1).

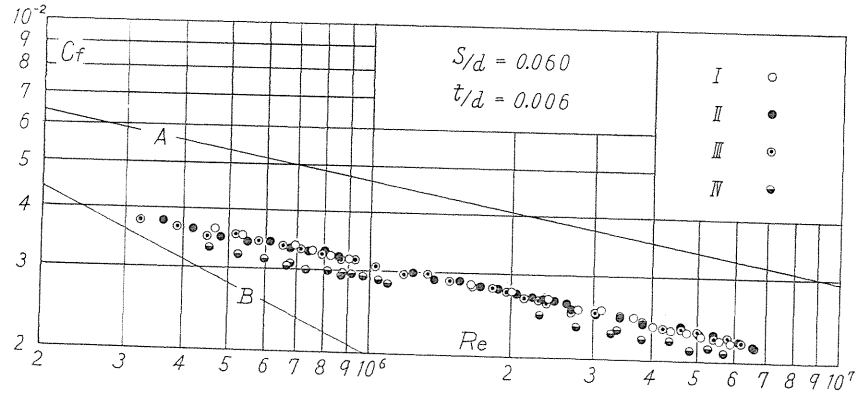

FIG. 11 (b). Results for concentrically bladed disc in smooth vessel (2).

the minimum value of C_f. Fig. 11 (a), (b) are the results of bladed disc in smooth vessel for $s/d=0.004$ and 0.060, respectively. Almost all experimental lines are in parallel with the theoretical line A. For a small clearance as in Fig. 11 (a), C_f decreases in turn from I to IV. For a large clearance as in Fg. 11 (b), C_f of I, II, III falls almost on a single line, thus there is little influence from the arrangement of disc blades.

3.4. Effects of radial blades

3.4.1. Experiments of bladed disc in smooth vessel

The experiments were carried out for various heights of $h=3.0$, 6.0, 12.0 mm. Fig. 12 shows the result with $h=6.0$ mm, and $Z=2$, 4, ..., 64 respectively. Here the axial clearance ratio s/d is taken as the parameter. Broken lines in Fig. 12 (a) indicate the results of smooth disc in vessel as the standard value. Transitional region from a laminar flow region to a turbulent which occurred in the experiments of the rough surface cannot be seen here. Then the relation between C_f and R_e is given by the following expression,

$$C_f=\alpha\cdot R_e^{-0,1575} \tag{5}$$

where α is a function of height of blade: h, number of blade: Z, axial clearance ratio s/d, etc. Table 3 shows the value of α of $s/d=0.01$. For example, the value of α of $h=3.0$ mm, $Z=16$ is equal to the value of $h=6.0$ mm, $Z=4$.

TABLE 3. Values of α (s/d=0.01)

$h\rightarrow$	h mm		
$Z\downarrow$	3.0	6.0	12.0
2	0.035	0.043	0.055
4	0.040	0.048	0.058
8	0.046	0.055	0.064
12	0.048	—	—
16	0.048	0.056	0.066
32	0.053	0.057	0.064
46	0.046	0.055	0.065

In Fig. 12, experimental results of a roughly grained disc in smooth vessel are shown by marks × ($i/d=1.34\times10^{-3}$). In the turbulent flow region, the inclination of these points in the relation of C_f-R_e is equal to that of the bladed disc. Although the experiments are carried out when the rough grains are laid on both surfaces of the disc, the chain line in Fig. 12 (a) is converted into the case where there are rough grains only on one side of disc. This line coincides generally with the results of bladed surface for $h=3.0$ mm, $Z=2$.

Fig. 13 shows the relation between C_f and s/d with parameter Z. The Symbol ⊖ indicates the results of smooth surface. In experiments of the smooth surface, C_f takes a minimum value when $s/d=0.005$, and in the bladed sutface of $h=3.0$, 6.0 mm, C_f takes a minimum value when $s/d\fallingdotseq0.01$, but the auther was unable to find a minimum value of C_f when $h=12.0$ mm. In $s/d\geqq0.01$, all C_f increase gradually with s/d. When $h=3.0$ mm and $Z=64$, the inclination of C_f-s/d curves is especially large as shown in Fig. 13 by broken curves.

Fig. 14 shows the relation between C_f and Z with parameter h. When $h=12.0$ mm, C_f is constant over $Z=16$, there is a tendency that C_f takes a maximum value with decrease of h. Fig. 13 and Fig. 14 are both the results of $R_e=10^6$.

3.4.2. Experiments of smooth disc in bladed vessel

Fig. 15 shows experimental results of the smooth disc in a vessel having the

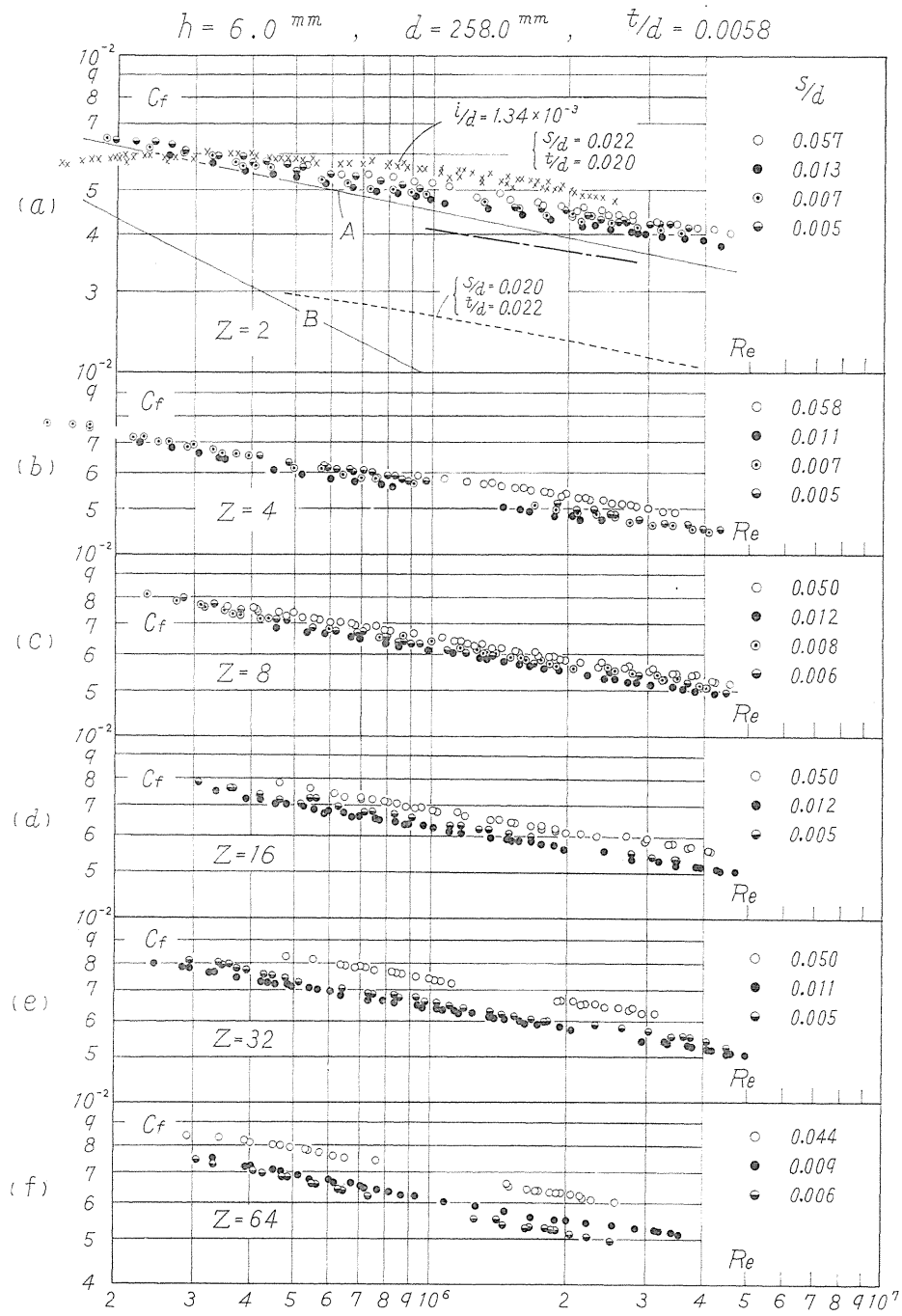

FIG. 12. Results for radially bladed disc in smooth vessel.

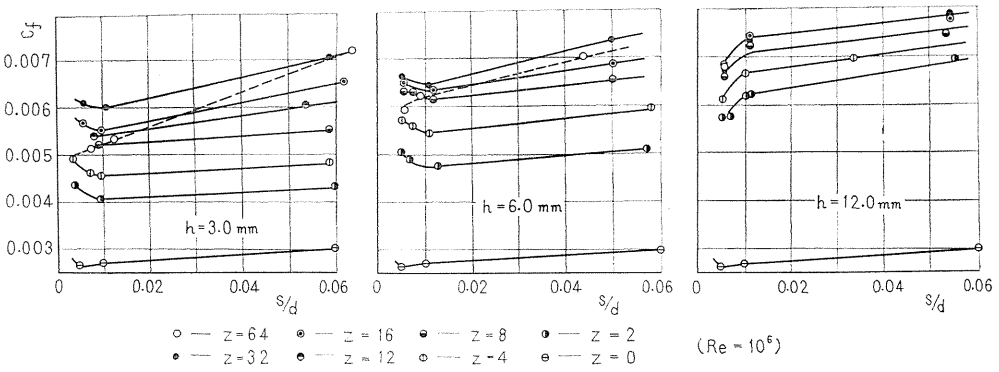

FIG. 13. Curves $C_f - s/d$.

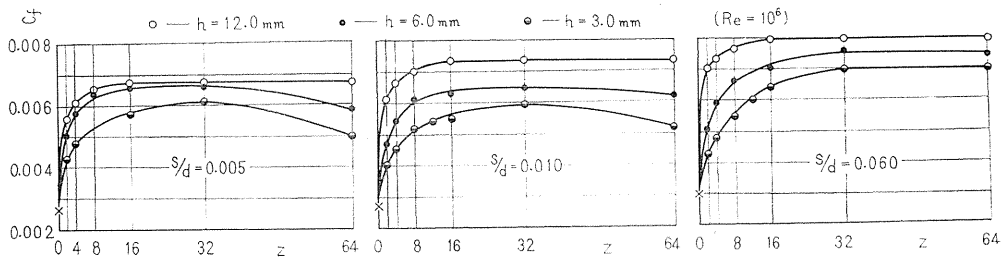

FIG. 14. Curves $C_f - Z$.

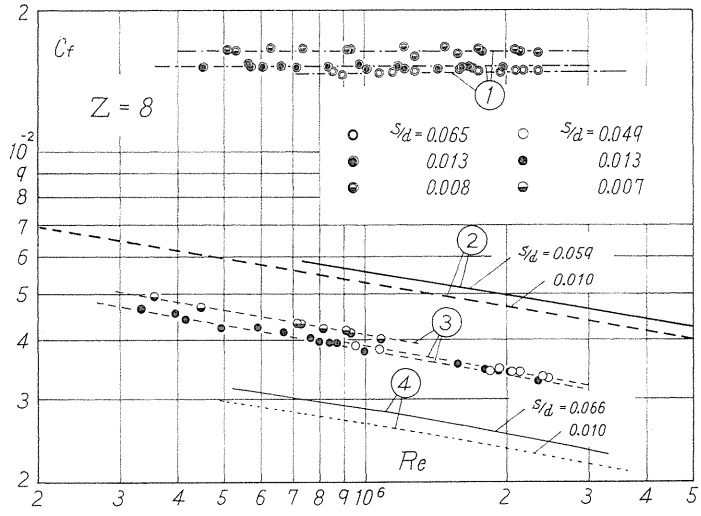

FIG. 15. Results for smooth disc in bladed vessel and bladed disc in bladed vessel (t/d=0.006, h=3.0 mm).

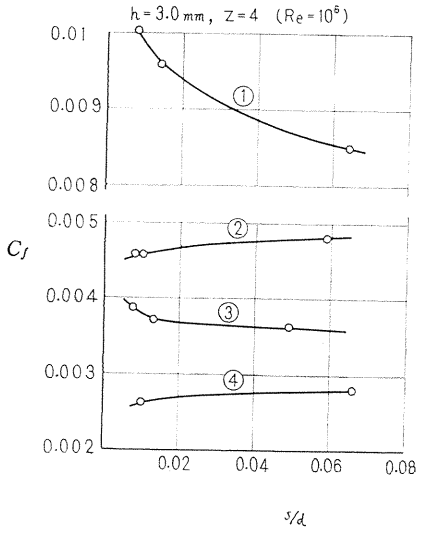

FIG. 16. Influences of axial ciearances.

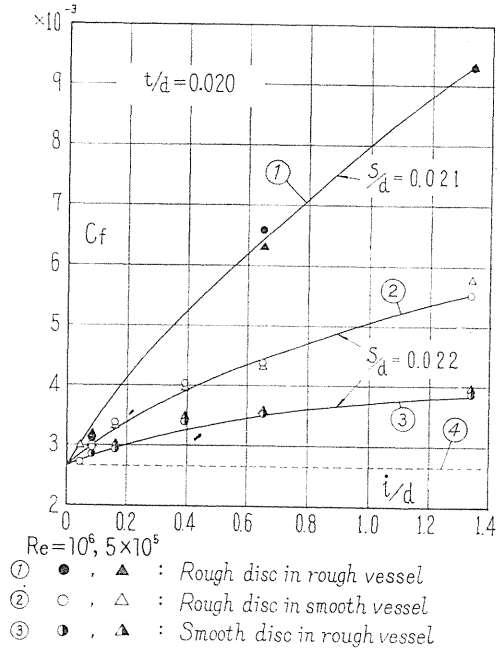

FIG. 17(a). Curves $C_f - i/d$.

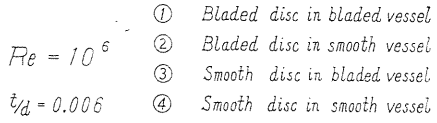

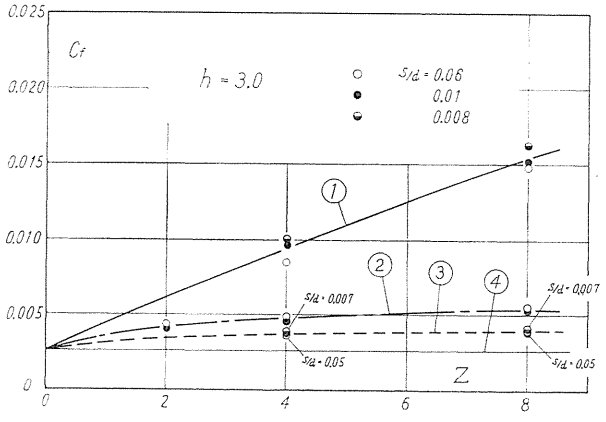

FIG. 17 (b). Curves $C_f - Z$.

rectangular blades on its one side ($h=3.0$, 6.0 mm, $Z=4$, 8) The results are shown with marks ○, ◉, ◒ by the symbol ③. Comparing these results with the results of bladed disc in smooth vessel (symbol ②) and smooth disc in smooth vessel (symbol ④), C_f-R_e lines of ③ lie between ② and ④, and this tendency coincides with the experimental results of sand grains. The value of C_f increases for a decreasing of s/d and this fact will be again shown in Fig. 16 later.

3.4.3. Experiments of bladed disc in bladed vessel

Experiments were carried out with the rectangular blades of the same kind and number both on one side of disc and on the vessel surfaces ($h=3.0$, 6.0 mm, $Z=2$, 4, 8). The results are shown in Fig. 15 mentioned previously, with points of the marks ◎, ◉, ◒ by the symbol ①.

The value of C_f increase considerably with the number Z and height of blade h, and the tendency of C_f is almost independent of R_e especially for a large number of blades ($Z\geqq 4$). In $Z=8$, C_f-R_e lines of $h=3.0$, 6.0 mm are almost horizontal. The influences of s/d are similar to the results of ③, i.e. C_f decreases for increasing of s/d, and the fact is remarkable in $Z=4$.

The experimental results discussed above were arranged on the relation between C_f and s/d as in Fig. 16. Where the symbols ①, ②, ③, ④ are the same as in the above figure respectively. In large clearances the influences of the blades of vessel are little, and then the curves ① and ②, ③ and ④ come near to one another, but in small clearances, ② and ③ tend to approach each other.

Lastly, the relations between C_f and i/d, C_f and Z are shown in Fig. 17 with the symbols ①, ②, ③, ④ as above. The following relations hold for the increment C_{f_1} (difference between ① and ④) and the increment C_{f_2} (difference between ② and ④) and the increment C_{f_3} (difference between ③ and ④),

$$C_{f_1} \fallingdotseq 2\, C_{f_2} \fallingdotseq 4\, C_{f_3} \tag{6}$$

for grain surfaces,

$$C_{f_2} \fallingdotseq 2\, C_{f_3} \tag{7}$$

for bladed surfaces, and the increment of bladed disc in bladed vessel differs considerably from that in the case of rough surfaces.

Acknowledgment

The author expresses his appreciation to the late Dr. Y. Shimoyama, and thanks Prof. Dr. Y. Furuya and Prof. Dr. T. Yamamoto for their kind guidance and valuable advice throughout the investigation. He also thanks the members of Hydraulic Laboratory for their encouragements.

References

1) T. von Kármán: Z. AMM, Bd. **1**, S. 233 (1921).
2) Schultz-Grunow: Z. AMM, Bd. **15**, Ht. 4, S. 191 (1935).
3) K. Pantell: Forschung, Bd. **16**, Nr. 4, S. 97 (1949–50).
4) Fujimoto and Iwagaki: Trans. Soc. Mech. Engrs. Japan, Vol. **13**, No. 44, p. 180 (1947) and Vol. **14**, No. 47, p. 44 (1948).
5) J. W. Daily and R. E. Nece: Trans. ASME Series D, Vol. **82**, No. 1, p. 217 and No. 3, p. 553 (1960).